

Supplemental Information

**Understanding the Stabilization Effect of the Hydrrous IrO_x
Layer formed on Iridium Oxide Surface during the Oxygen
Evolution Reaction in Acid**

Jun Qi,^a Muzhi Yang,^b Huiyan Zeng,^a Yabin Jiang,^a Long Gu,^a Wenguang Zhao,^c Zhongfei Liu,^a Tianhui Liu,^d Chunzhen Yang^{*a,d}, Rui Si^{*a,d}

^aSchool of Materials, Sun Yat-Sen University, Shenzhen, 518107, P. R. China

^bSun Yat-Sen University Instrumental Analysis & Research Center, Guangzhou, 510275, P. R. China

^cPeking University ShenZhen Graduate School, Shenzhen, 518107, P. R. China

^dSynchrotron Radiation Facility Division, Institute of Advanced Science Facilities (IASF), Shenzhen, 518108, P. R. China

*Correspondence to: yangchzh6@mail.sysu.edu.cn; sirui@mail.sysu.edu.cn

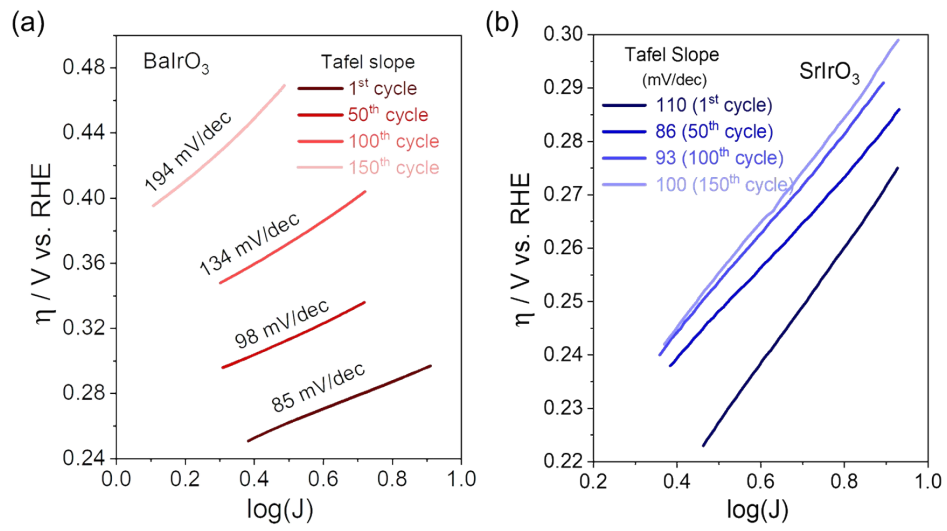


Figure S1 Evolution of Tafel curves of BaIrO₃ (a) and SrIrO₃ (b) after certain number of electrochemical cycling.

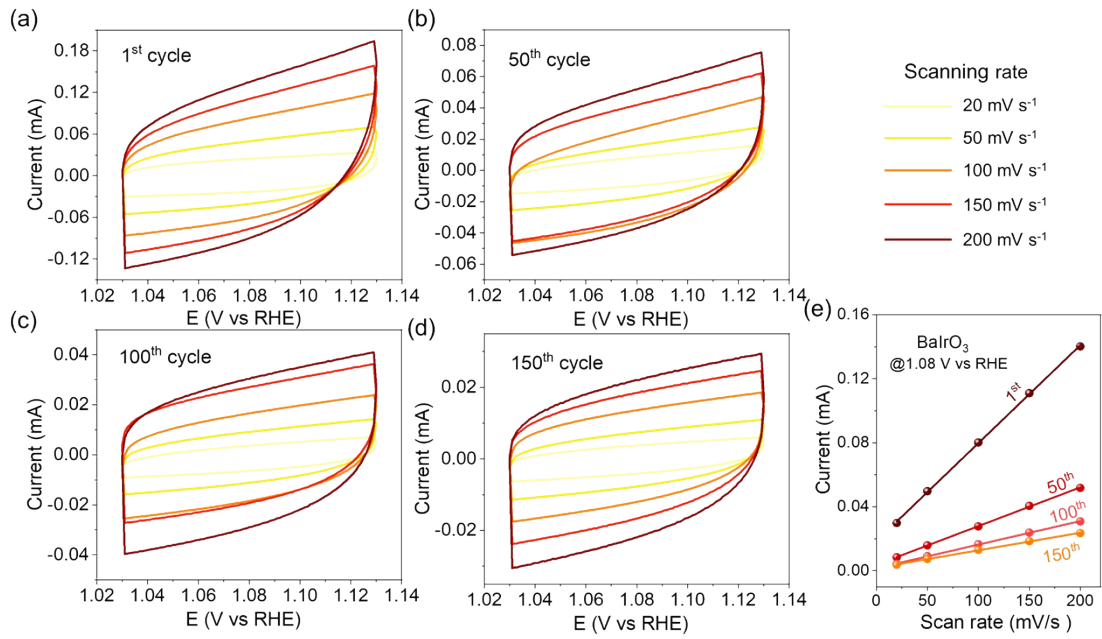


Figure S2 Cyclic voltammograms and charging currents for DL capacitance measurements in BaIrO₃. The electric double-layer capacitance was calculated by fitting the curve of charging current (at 1.08 V vs RHE) and scan rate.

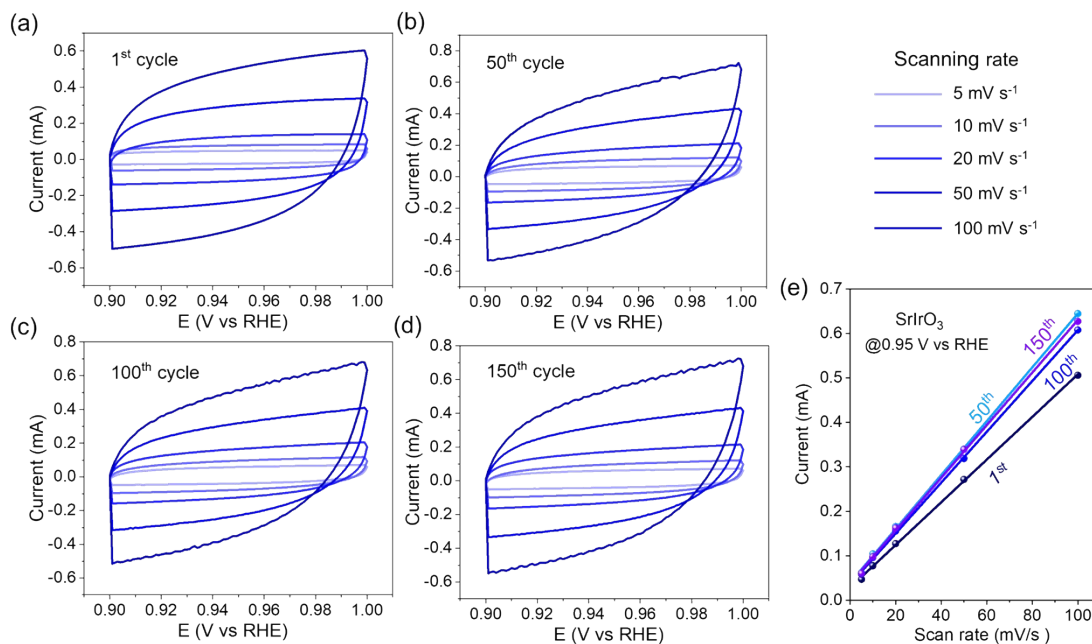


Figure S3. Cyclic voltammograms and charging currents for DL capacitance measurements in SrIrO₃. The electric double-layer capacitance was calculated by fitting the curve of charging current (at 0.95V vs RHE) and scan rate.

The electric double-layer capacitance (C_{dl}) was calculated from the scan-rate dependent CVs in non-Faradaic potential region with various scan rates.¹ The C_{dl} was calculated according to the equation $i_c = \nu C_{dl}$, where C_{dl} is the double-layer capacitance (mF), ν is the scan rate (mV s⁻¹), i_c is charging current (mA). Thus, a plot of i_c as a function of ν yields a straight line with a slope equal to C_{dl} .

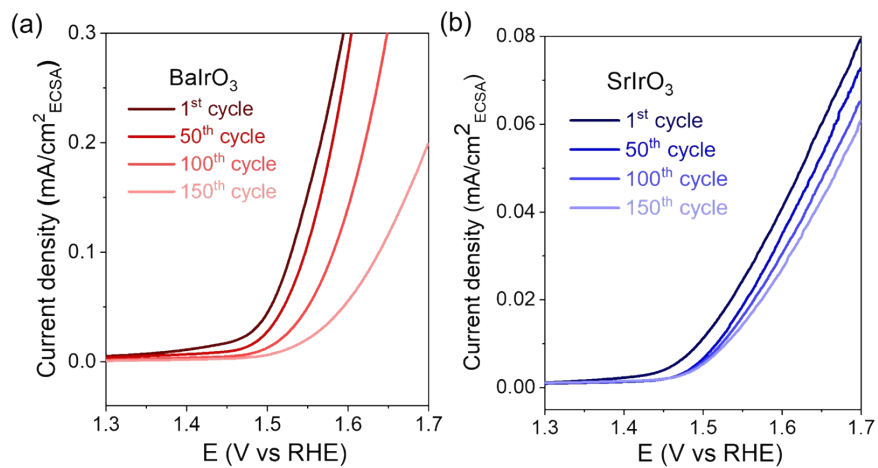


Figure S4. CV profiles of 1st, 50th, 100th, 150th cycle for BaIrO₃ and SrIrO₃ with currents normalized by the ECSA.

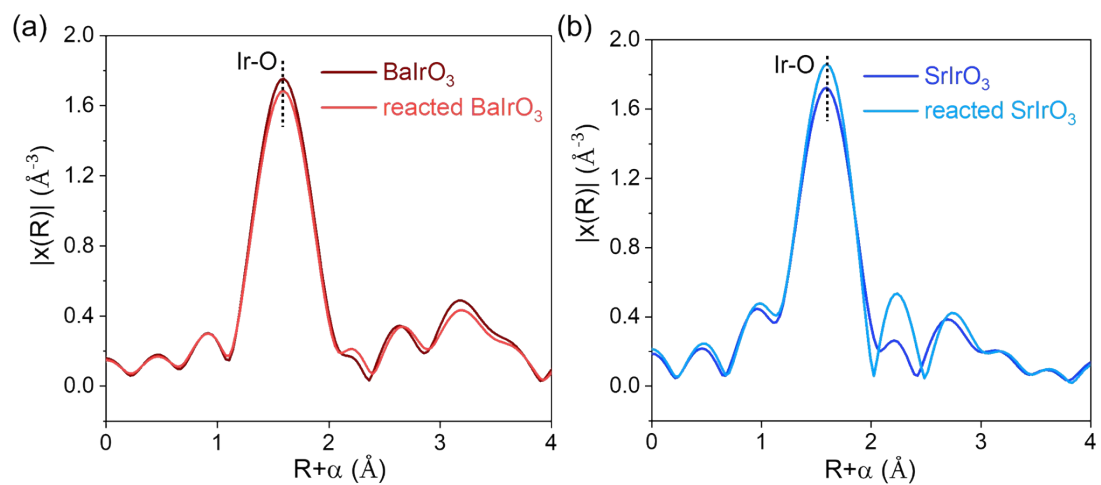


Figure S5. Comparison of the Ir L_{III} -edge EXAFS curves for the pristine and reacted BaIrO_3 (a) and SrIrO_3 (b) with a k range of $3 \leq k \leq 10 \text{ \AA}^{-1}$. These data are k^2 -weighted and not phase-corrected.

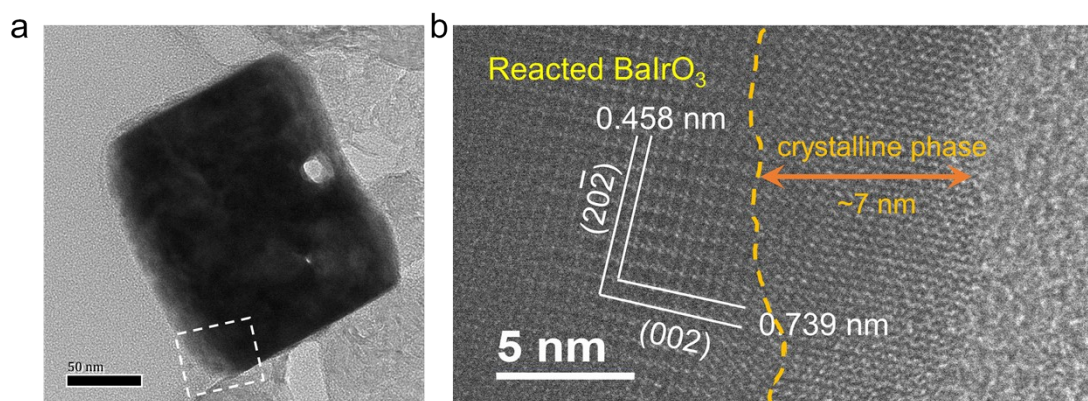


Figure S6. TEM images of reacted BaIrO₃. (a) A typical oxide particle after electrochemical cycling, (b) high-resolution TEM image showing the crystalline structure at the exposed region.

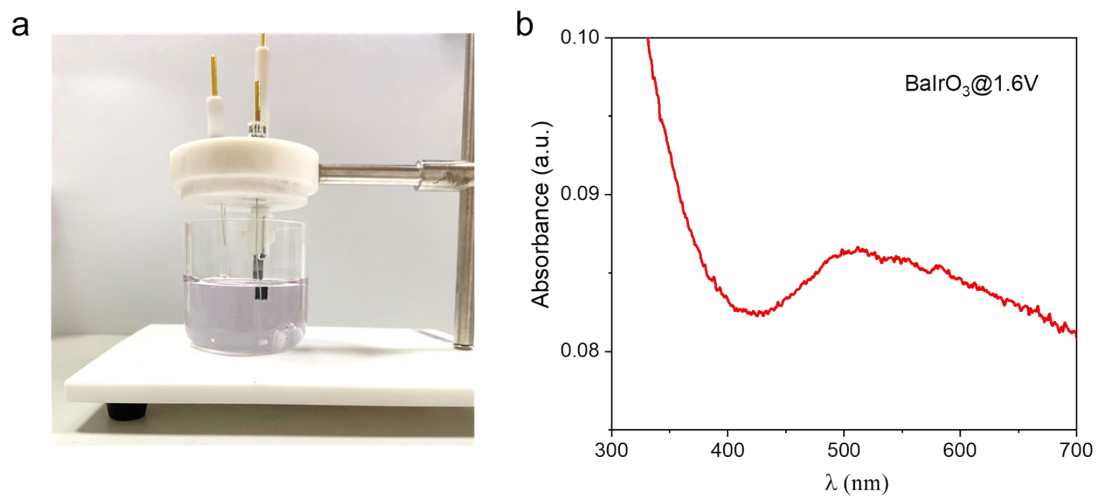


Figure S7. (a) Reaction setup of BaIrO₃ catalyst after holding at 1.6 V vs. RHE for 12 hours, (b) corresponding UV-Vis spectrum of the reacted H₂SO₄ electrolyte.

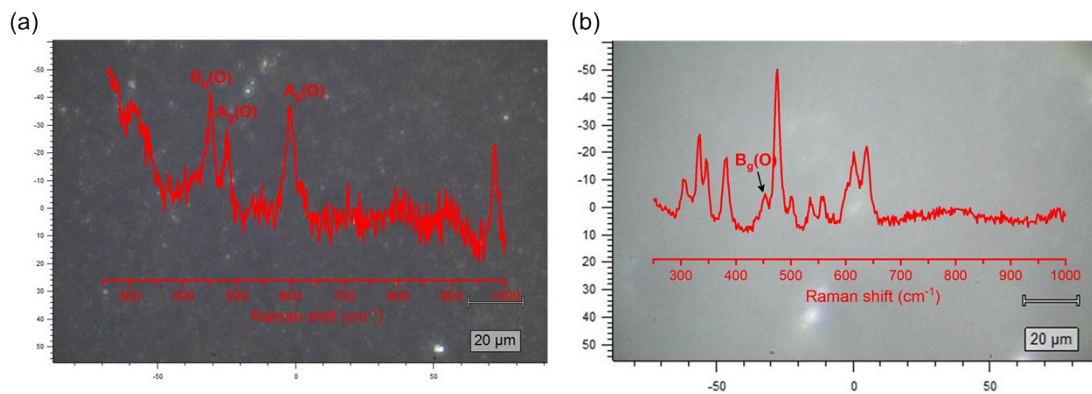


Figure S8. The optical photos of the initial (a) and reacted BaIrO₃ (b) after holding at 1.7 V vs RHE taken from the *operando* Raman experiments. Insets are the corresponding Raman spectra.

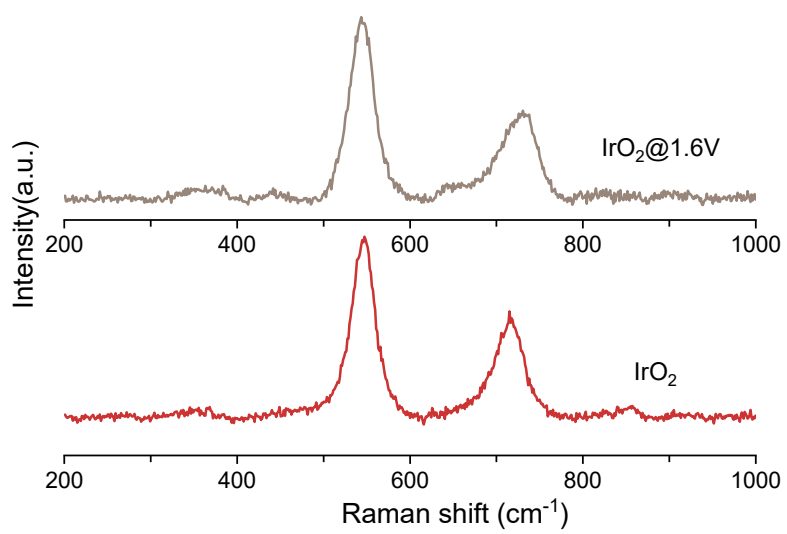


Figure S9. The Raman spectra of pristine and reacted IrO₂ after holding at 1.6 V vs RHE for 12h.

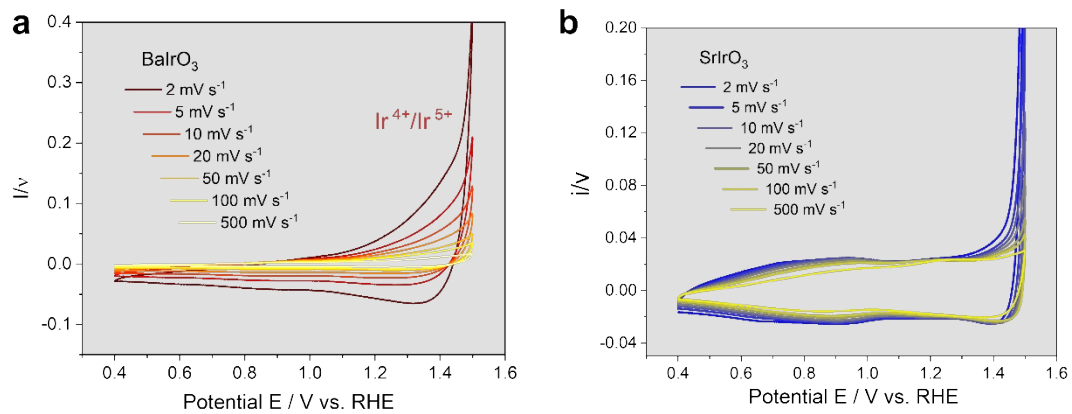


Figure S10. Cyclic voltammograms of BaIrO_3 and SrIrO_3 at different scan rates in $0.5 \text{ M H}_2\text{SO}_4$.

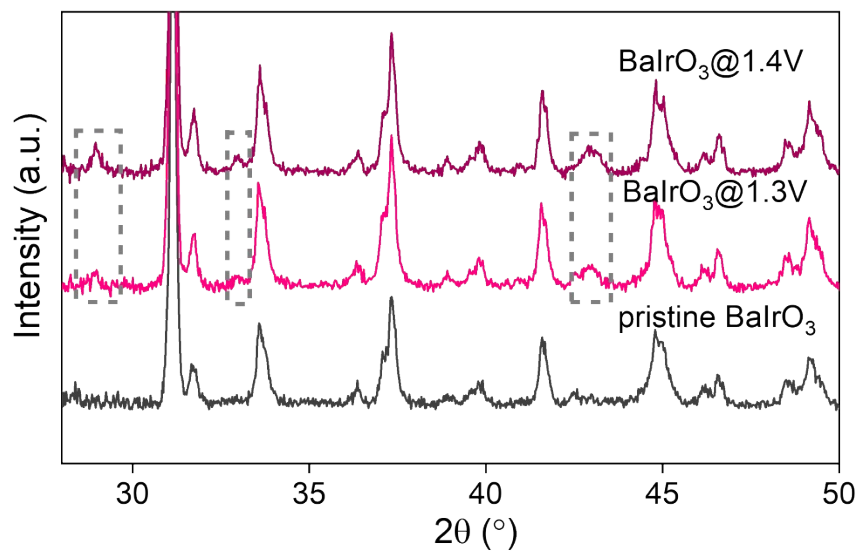


Figure S11 Evolution of XRD patterns of pristine BaIrO₃ and reacted BaIrO₃ after holding at 1.3 and 1.4 V vs. RHE in 0.5 M H₂SO₄ solution for 12 hours.

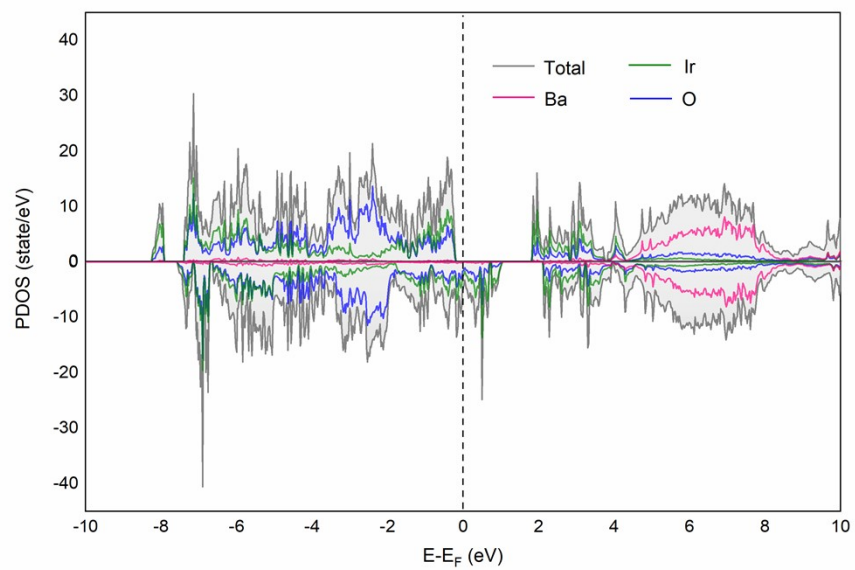


Figure S12. PDOS of BaIrO₃ as calculated by DFT in which the Fermi level is 0 eV.

Table 1. The parameters from the Rietveld refinement of BaIrO₃ and SrIrO₃.

Compound	Space group	a (Å)	b (Å)	c (Å)	α (°)	β (°)	γ (°)	V _{unit-cell} (Å ³)	R _p	R _{wp}
BaIrO ₃	C 1 2/m 1	10.011	5.763	15.135	90	103.18	90	850.15	7.9	10.1
SrIrO ₃	C 1 2/c 1	5.620	9.620	14.169	90	93.21	90	762.73	6.2	8.0

Reference

- [1] McCrory, C. C.; Jung, S.; Peters, J. C.; Jaramillo, T. F., Benchmarking heterogeneous electrocatalysts for the oxygen evolution reaction. *J Am Chem Soc* **2013**, *135* (45), 16977-16987.